Crystal and chemical anisotropy effects in AE2Zn2N2, (AE = Ca, Sr, Ba) from ab initio

Samir F. Matar, Jean Etourneau, Naïm Ouaini

Solid State Sciences, accepted Nov 2014

Crystal and chemical anisotropy effects in AE_2ZnN_2, (*AE* = Ca, Sr, Ba) from ab initio.

Samir F. Matar[a, b] *, Jean Etourneau [a, b], Naïm Ouaini [c]

[a]CNRS, ICMCB, UPR 9048, 33600 Pessac, France

[b]Université de Bordeaux, ICMCB, UPR 9048, 33600 Pessac, France

[c]Université Saint Esprit de Kaslik, CSR-USEK, CNRS_L, Jounieh, Liban

*Email: matar@icmcb-bordeaux.cnrs.fr ; abouliess@gmail.com

Keywords: Nitrides. DFT. Compressibility. Cohesive energy. Elastic properties. Bonding.

Abstract:

In the tetragonal ternary nitrides AE_2ZnN_2 (*AE* = Ca, Sr, Ba), Zn has a rare linear coordination with nitrogen (N–Zn–N) along the *c* axis and N is located in an AE_5Zn–like octahedron. Such features lead to original anisotropic crystal and chemical bond effects addressed herein with DFT-GGA based methods accounting for the cohesive energies, the energy volume equations of state EOS, the elastic constants and the properties of chemical bonding. Along *AE* = Ca, Sr, Ba an increasing overall compressibility under hydrostatic pressure is inferred from the respective EOS's, but the elastic constants C_{ij} exhibit highly anisotropic features with large magnitudes of C_{33} along the tetragonal *c* axis versus smaller C_{11}= C_{22} along *a*, *b*. Decreasing C_{33}-C_{11} along the title compounds signals decreasing anisotropy. The three ternaries are calculated as small gap insulators in agreement with experimental results of conductivity. The chemical bonding characterizes strong Zn-N bonds versus weaker *AE*–N thus reflecting the crystal anisotropy.

1. Introduction and context.

Nitrides offer a broad range of chemical compounds with interesting physical properties mainly related with the covalent character of the host elements with nitrogen. This is illustrated for instance by the extreme hardness of light element nitrides within the B-C-N diagram such as the cubic boron nitride c-BN which replaces diamond in many tooling machines either as bulky materials or more recently as thin films [1], the ternary BC_2N [2] and the theoretically devised $C_{11}N_4$ [3]. Also the refractory character of transition metal mononitrides [4] and of SiCN ceramics [5] is of large interest in industry.

AE_2ZnN_2 (AE = Ca, Sr, Ba) ternaries were synthesized by DiSalvo group in the 1990's [6,7]. They form the first nitrides with the A_2HgO_2 (A= alkaline element) archetype prepared earlier by Hoppe and Röhrborn in 1964 [8]. The structure is body centered tetragonal with large c/a ratio of 3.1 – 3.5. It is characterized by a rare linear coordination of Zn to nitrogen: N...Zn...N and an *AE5Zn* irregular octahedron surrounding nitrogen with five long $d_{AE\text{-}N}$ and one short $d_{Zn\text{-}N}$ (cf. Fig. 1). This leads to ionocovalent compounds with chemical generic formulation: $2AE^{2+}\{N...Zn...N\}^{4-}$ where ZnN_2^{4-} is a complex linear anion. The directional N...Zn...N bonds along the tetragonal c-axis are likely to exhibit original anisotropic mechanical as well as peculiar chemical bonding effects leading to specific physical properties which are examined herein by calculating the electronic structure and energy derived quantities of the three compounds within the quantum mechanical framework of the density functional theory DFT [9]. Two computational methods were used in a complementary manner. The Vienna ab initio simulation package (VASP-PAW) code [10,11] allows accurate protocols of geometry optimization, cohesive energies, energy volume equations of state (EOS) and the calculation of the complete set of elastic constants. Then a full account of the electronic structure and of the properties of chemical bonding (not implemented in VASP) is done with full potential all electrons augmented spherical wave (ASW) method [12,13]. The DFT exchange-correlation XC effects were considered following the generalized gradient approximation (GGA) according to the scheme of Perdew, Burke and Ernzerhof (PBE) [14]. Details on the methods can be found in a recent work [15] and therein references.

2. Geometry optimization and energy based results

Geometry optimization and cohesive energies.

Starting from the experimental structure parameters of AE_2ZnN_2, *AE* = Ca, Sr, Ba [6,7] given in Table 1, unconstrained geometry optimization runs were carried out. In all three ternary compounds the tetragonal symmetry in $I4/mmm$ space group was preserved after successive calculations with increasing precision of the Brillouin zone integration. As shown in Table 1, the fully relaxed structure parameters are found close to the starting ones and the shortest interatomic distances are in fair agreement with experiment. The distance *d*(Zn–N)= 1.84 Å is almost constant throughout the series and smaller than *d*(*AE*–N) which ranges from 2.4 Å (*AE* = Ca), to 2.54 Å (*AE* = Sr) and 2.60 Å (*AE* = Ba) whence the volume increase (Table 1). The calculated volumes present smaller magnitudes than experimental values but it will be shown in next paragraph that a better agreement is obtained from the energy-volume equations of states (EOS) fit values (cf. Fig. 2).

The last lines of Table 1 report the total and cohesive energies. The latter are obtained from:

$E_{coh.} = E_{total}$(compound) - Σ E(constituents) for one FU.

The energies of the constituents were calculated in their ground state structures using available PAW-GGA potentials: FCC for *AE* with E_{Ca} (including *p* semi-core state) = -1.954 eV/atom, E_{Sr} (including *s* and *p* semi-core state) = -1.677 eV/atom E_{Ba} (including *s* and *p* semi-core state)= -1.911 eV/atom; hexagonal E_{Zn} = -1.250 eV/atom and N_2 in a large cubic box, E_{N2}. = -16.136 eV. The trend of decreasing cohesive energies along the series results not from the Zn-N constant separation but from the increasing *AE*-N distance as shown above.

Energy-volume equations of states

In view of the increasing lattice constants and subsequently of the volume from Ca to Sr then to Ba, it becomes relevant to examine the structure response to volume change by obtaining the energy-volume equations of state (EOS) for the three compounds. This proceeds from the *E,V* (energy-volume) set of calculations around the minima found from the geometry optimization (Table 1). The resulting $E = f(V)$ curves are shown in Figs. 2.

They have a quadratic variation which can be fitted with Birch EOS up to the 3rd order [16]:

$$E(V) = E_o(V_o) + (9/8)V_oB_o[([(V_o)/V])^{[2/3]}B'-1]^2 + [9/16]B_o(B'-4)V_o[([(V_o)/V])^{[2/3]}-1]^3,$$

where E_o, V_o, B_o and B' are the equilibrium energy, the volume, the bulk modulus and its pressure derivative, respectively. In the inserts χ^2 values designating the goodness-of-fit are small enough to provide confidence to the fit results especially for the close values of equilibrium energies E_0 to the ones obtained by energy optimization and for the volumes V_0 which show a better agreement with the experiment than the geometry optimization results (Table 1). All three B' values are close to 4, i.e. within range of usually obtained values [17]. The respective B_o values have small magnitudes and they are found in the range of compressible metals and alloys [17] i.e., far from the magnitudes found in ultra-hard nitrides as BC_2N and $C_{11}N_4$ whose bulk modules are in the range of 300–400 GPa [2,3]. Also the B_0 values decrease within the series: The compound with the largest volume (*AE* = Ba) becomes most compressible under hydrostatic pressure.

However these observations do not provide sufficient information on the effects of the structure anisotropy reflected by the linear N…Zn…N entities along the *c*–axis . A detailed description can be provided through the calculation of the set of elastic constants C_{ij}

Elastic constants

The elastic properties are determined by performing finite distortions of the lattice and deriving the elastic constants from the strain-stress relationship. In tetragonal symmetry there are six independent elastic stiffness constants C_{11}= C_{22}, C_{33}, C_{44}, C_{66}, C_{12}, and C_{13}. Most encountered compounds are polycrystalline where monocrystalline grains are randomly oriented so that on a large scale, such materials can be considered as statistically isotropic. They are then completely described by the bulk modulus *B* and the shear modulus *G*, which may be obtained by averaging the single-crystal elastic constants. The most widely used averaging method of the elastic stiffness constants is the method of Voigt [18] based on a uniform strain. The calculated elastic constants are given in Table 2. All C_{ij} values are positive and their combinations: $C_{11} > C_{12}$, $C_{11}C_{33} > C_{13}^2$ and $(C_{11}+C_{12})C_{33} > 2C_{13}^2$ obey the rules pertaining to the mechanical stability of all three title compounds. Focusing on C_{11}, C_{22} and C_{33} translating stresses along the three orthogonal axes, it can be observed that while $C_{11} = C_{22}$ (as expected in tetragonal symmetry where $a = b$) a much larger C_{33} (along

the *c* axis) magnitude is found for all three compounds whereby the crystal lattice should be harder along the *c*–axis along which the N–Zn–N linear entities with short Zn–N connections are aligned, so that the Ca_2ZnN_2 compound presents an implicate hardness closer to the range of covalent nitrides [2,3,8]. Oppositely it is soft along the *a*, *b* directions. However the difference between C_{11} and C_{33} decreases along the series. This can be interpreted in terms of largest anisotropy for Ca_2ZnN_2 and the lowest anisotropy for Ba_2ZnN_2.

The bulk (B_V) and shear (G_V) modules following Voigt are formulated as:

$$B_V = 1/9\ \{2(C_{11} + C_{12}) + 4C_{13} + C_{33}\} \text{ and}$$

$$G_V = 1/30\ \{12C_{44} + 12C_{66} + C_{11} + C_{12} + 2C_{33} - 4C_{13}\}$$

The numerical values (Table 2) show good agreement of B_V with B_0 obtained from EOS fits (Fig. 2), thus showing the complementary description of the compounds in the two approaches. The shear modulus which defines the rigidity of the material is significantly lower. The Pugh's G_V/B_V ratio [19] is an indicator of brittleness or ductility for $G_V/B_V > 0.5$ and $G_V/B_V < 0.5$, respectively. G_V/B_V ratio is found to decrease from 0.57 in Ca_2ZnN_2 to 0.43 in Ba_2ZnN_2, indicating reduced brittleness along the series. Note that for Ba_2ZnN_2 the G_V/B_V ratio approaches the value observed experimentally for the coinage metals Ag, Pt, or Au which possess G_V/B_V ratios in the range of 0.4-0.2 [20].

To conclude on this section, it has been shown that along *AE* = Ca, Sr, Ba, peculiar properties pertaining to decreasing cohesive energies and incompressibilities as well as decreasing anisotropy characterize the AE_2ZnN_2 compounds.

3. Electronic structure and chemical bonding

In as far as the calculated structure parameters are close to experiment for AE_2ZnN_2 (Table 1) we use the latter for the analysis of the electronic structure with all electrons calculations with the full potential ASW method [12,13]. In the minimal basis set used by the ASW method the valence states and the matrix elements were constructed using partial waves up to $l_{max}+1 = 3$ for *AE* and Zn and $l_{max}+1 = 2$ for N. Also the Zn($3d^{10}$) filled subshell was not considered as part of the valence basis set of Zn and replaced by $4d^0$. The chemical bonding for pair interactions is analyzed qualitatively using the crystal orbital

overlap populations COOP based on the overlap matrix elements S_{ij} [21]. In the plots positive, negative and zero magnitude COOP indicate bonding, anti-bonding and non bonding interactions respectively.

At self consistent energy and charge convergence the transfer of electrons follows the trend discussed above of positively charged *AE* and Zn and negatively charged N but does not translate the ionic of $2AE^{2+}$ $\{N...Zn...N\}^{4-}$ which is a formal picture rarely observed in the solid state. The site projected densities of states (PDOS) are shown in Fig. 3. The zero energy along the *x*–axis is with respect to the top of the valence band (VB) E_V and the compounds are insulating -or small gap semi-conductors- with a ~2 eV band gap for Ca and Sr compounds and a reduced gap of ~1 eV for the barium compound. For Ca_2ZnN_2 the result agrees with the experimental observations of conductivity and magnetic measurements but no gap magnitude was provided [6].

As a general feature the lower part of the VB around -12 eV is occupied by N 2*s* states which show similar shape with the PDOS of *AE* and Zn. This is also observed for the *p*-block from -4 to E_V. The large magnitude of AE and N PDOS as with respect to Zn arises from their twice larger number but the similar PDOS shapes are signatures of the quantum mixing between the valence states leading to the chemical bonding. The conduction band (CB) in the range of 2-6 eV is dominated by the empty *AE* states resulting from the positive ionization. In the case of barium, the broad band within the CB due to *s*–like has the main effect of reducing the band gap as with respect to the Ca dn Sr compounds. Also the *p*-block PDOS show a progressive localization along the series especially for the intense peak at ~2eV relative to N-p_z as inferred from a projection of N-*p* PDOS.

In view of the coordination polyhedron of N in *AE5Zn* like octahedron (cf. Fig. 1) and of the short Zn-N distance versus *AE*-N ones, Figs. 4 show the COOP for the *AE*-N and Zn-N different interactions. In order to establish comparisons, one atom of each kind is considered in the plots. The whole VB is of bonding nature with positive COOP magnitude and the CB is antibonding thus illustrating the largely negative cohesive energies (Table 1).

Clearly the Zn–N bond is dominating over *AE*-N in the *p*-block just below E_V and small bonding *s*-like COOP contribution, larger for *AE*-N is found at the lower part of the VB. The sharp peak at -2 eV corresponds to the directional N-p_z states. Such anisotropic bonding

is at the origin of the large C_{33} elastic constant identified in the three compounds. They provide brittle mechanical properties which are reduced upon volume increase along the series.

To conclude on this section the results obtained from the geometry optimization are complemented by a description of the title compounds as insulating with ~2eV band gap. The crystal anisotropy is well reflected by the larger Zn-N versus *AE*-N bonding.

Acknowledgement.

Computations were conducted on the MCIA-University of Bordeaux computers.

Support from *Conseil Régional d'Aquitaine* is gratefully acknowledged.

References

[1] C. B. Samantaray, R. N. Singh, International Materials Reviews 50, 313 (2005).

[2] M. Mattesini, S.F. Matar, International Journal of Inorganic Materials 3, 943 (2001).

[3] M. Mattesini, S.F. Matar, Phys. Rev. B 65 (7): Art. No. 075110 (2002).

[4] E. G. Gillan, R. B. Kaner, Inorg. Chem. 33, 5693 (1994)

[5] E. Betranhandy, L. Capou, S.F. Matar, C. El-Kfoury. Solid State Sci., 6, 315 (2004).

[6] M. Chern, F.J. Di Salvo, J. Solid State Chem. 88, 528 (1990).

[7] H. Yamane, F.J. Di Salvo, J. Solid State Chem. 119, 5375 (1995).

[8]. V. R. Hoppe, H-J. Röhrborn, Z. für anorg. allgemeine Chemie, 329, 110 (1964).

[9] P. Hohenberg, W. Kohn, Phys. Rev. B, 136 864 (1964) and W. Kohn, L.J. Sham, Phys. Rev. A, 140 1133 (1965).

[10] G. Kresse, J. Furthmüller, Phys. Rev. B 54 11169 (1996).

[11] G. Kresse, J. Joubert, Phys. Rev. B 59, 1758 (1999).

[12] A.R. Williams, J. Kübler, C.D. Gelatt Jr., Phys. Rev. B 19 6094 (1979).

[13] V. Eyert, Int. J. Quantum Chem., 77 1007 (2000).

[14] J. Perdew, K. Burke, M. Ernzerhof, Phys. Rev. Lett. 77 3865 (1996).

[15] S. F. Matar, B. Ourane, E. Gaudin, J-L. Bobet, A.F. Al Alam, N. Ouaini, Solid State Sci. 38, 1 (2014).

[16] F. Birch, J. Geophys. Res. 83 1257 (1978).

[17] S.F. Matar, Solid State Sci., 12 59 (2010).

[18] S. F. Matar, *Matériaux ultra-durs: Concepts et Modélisations*. Série *Techniques de l'ingénieur.* Eds. T. I. Sciences et Techniques. Paris. - AF 6630 (20 pp.), 2009.

[19] S. F. Pugh, Phil. Mag., 45, 823 (1954).

[20] S. Kamran, K. Chen, L. Chen, L. Zhao, J. Phys.: Condens. Matter., 20, 085221 (2008).

[21] R. Hofmann, Angew. Chem. Int. Ed. Engl., 26, 846 (1987).

Table 1. Calculated and experimental [4] (in parentheses) lattice and atomic parameters for AE_2ZnN_2, (AE = Ca, Sr, Ba). Space group $I4/mmm$ with Zn at ($2a$): 0,0,0, AE and N at $(4e)$: 0,0,z. Total electronic and cohesive energies are given as per formula unit (FU).

AE_2ZnN_2	AE = Ca	AE = Sr	AE = Ba
a (Å)	3.56 (3.58)	3.83 (3.86)	4.12 (4.15)
c (Å)	12.56 (12.66)	12.82 (12.93)	12.90 (13.05)
V (Å^3)	159.18 (162.26)	188.06 (192.65)	218.97 (224.75)
z_{AE}	0.303 (0.302)	0.342 (0.341)	0.348 (0.344)
z_N	0.147 (0.146)	0.144 (0.145)	0.143 (0.141)
$E_{Tot.}$ (eV)/FU	-25.47	-24.02	-23.75
$E_{coh.}$ (eV)/FU	-4.17	-3.27	-2.54

Table 2 AE_2ZnN_2, (AE = Ca, Sr, Ba: Elastic constants C_{ij} in GPa units and the bulk and shear modules.

AE_2ZnN_2	AE = Ca	AE = Sr	AE = Ba
C_{11} ; C_{22}	158.8	130.76	97.38
C_{12}	36.40	35.99	34.78
C_{13}	45.65	41.65	33.07
C_{33}	235.65	180.98	130.74
C_{44}	59.66	53.95	38.74
C_{66}	28.35	13.18	1.95
C_{33}-C_{11}	76.85	50.20	33.36
B_V	89.85	76.57	58.59
G_V	51.33	39.96	24.99
G_V/B_V	0.57	0.52	0.43

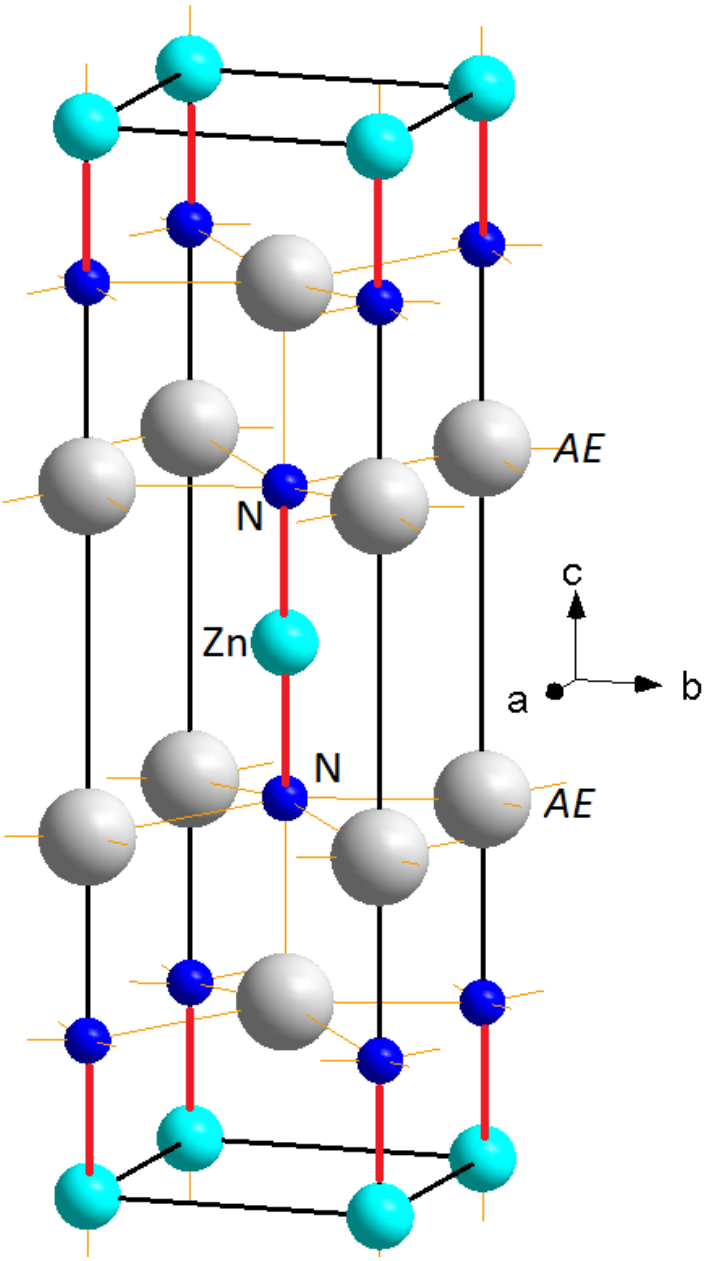

Fig. 1: Crystal structure of AE_2ZnN_2 (AE = Ca, Sr, Ba) family highlighting the linear N-Zn-N connections.

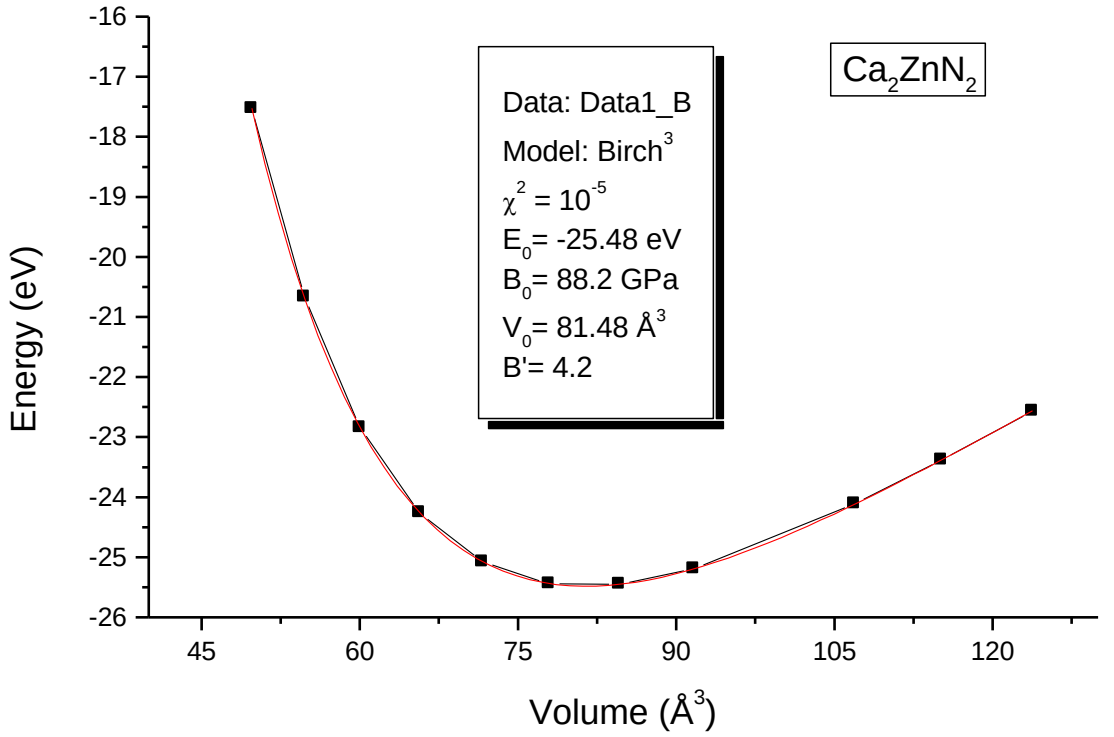
Ca2ZnN2
Data: Data1_B
Model: Birch3
χ2 = 10-5
E0= -25.48 eV
B0= 88.2 GPa
V0= 81.48 Å3
B'= 4.2
Energy (eV)
Volume (Å3)
-16
-17
-18
-19
-20
-21
-22
-23
-24
-25
-26
45
60
75
90
105
120

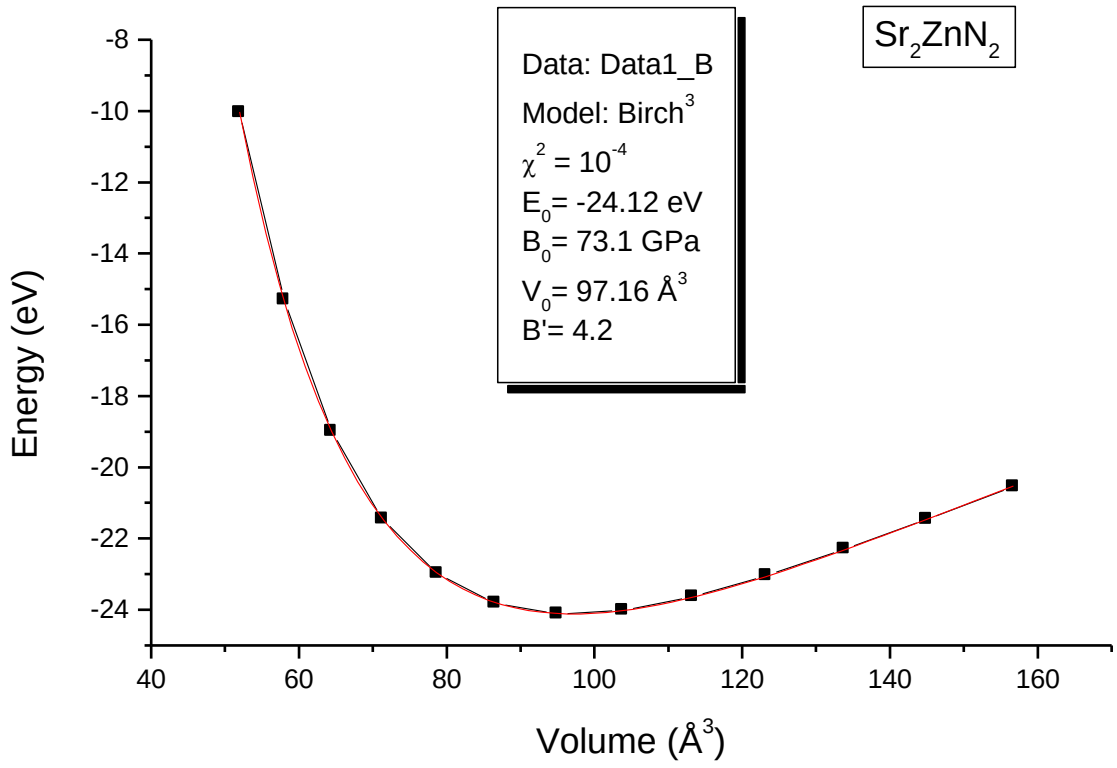
Sr2ZnN2
Data: Data1_B
Model: Birch3
χ2 = 10-4
E0= -24.12 eV
B0= 73.1 GPa
V0= 97.16 Å3
B'= 4.2
Energy (eV)
Volume (Å3)
-8
-10
-12
-14
-16
-18
-20
-22
-24
40
60
80
100
120
140
160

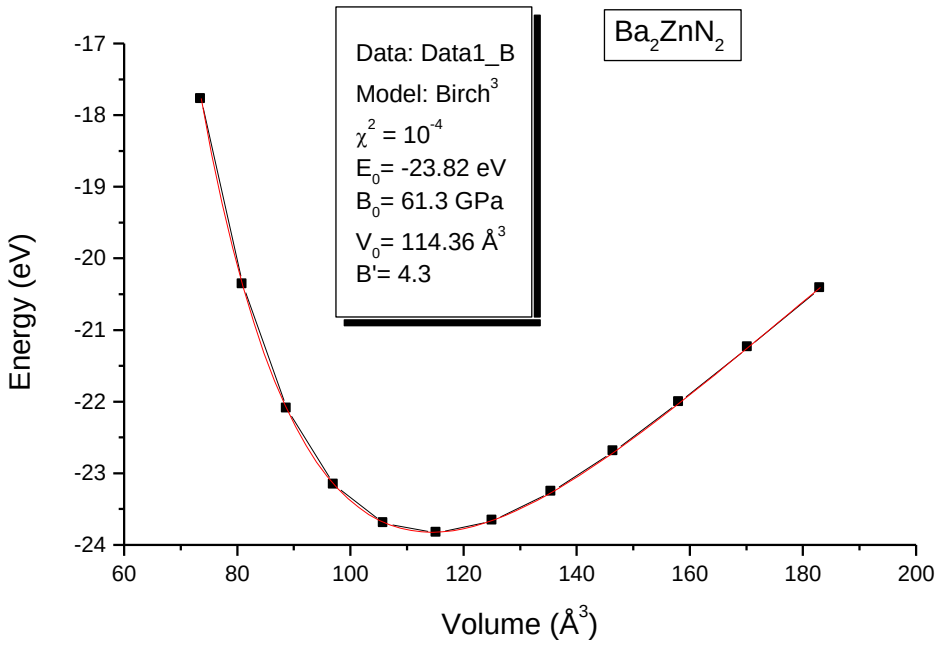

Fig. 2: AE_2ZnN_2 (*AE*= Ca, Sr, Ba). Energy volume curves and fit values (in the insert) from Birch 3rd order equation of state. χ_2: the goodness-of-fit.

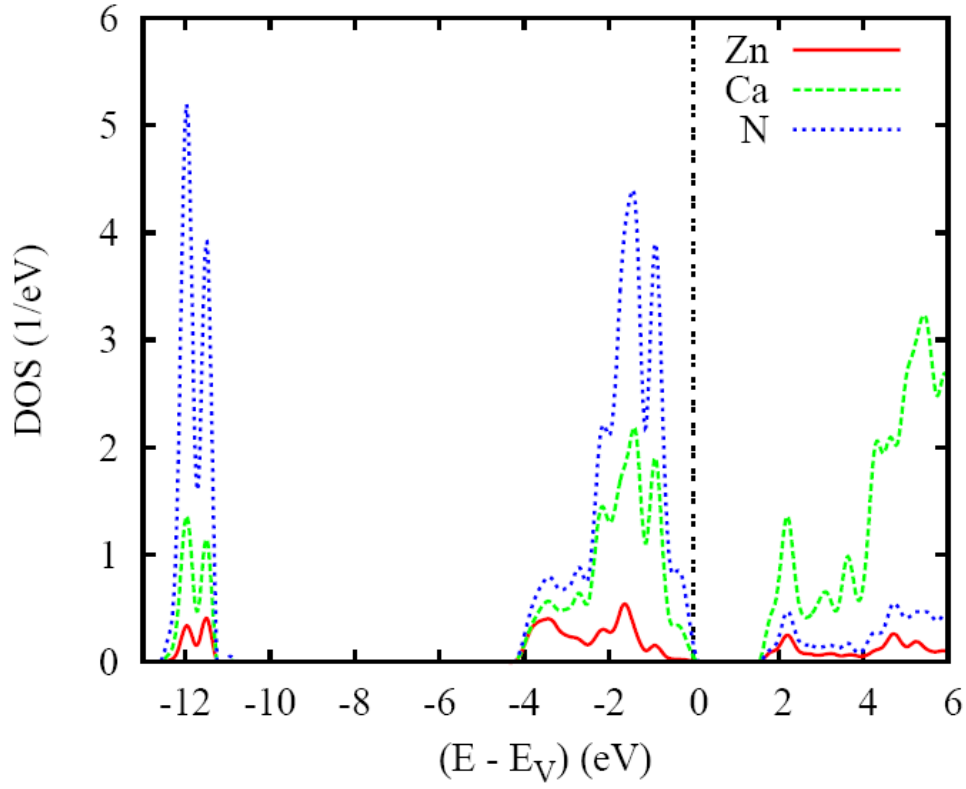
Zn
Ca
N
DOS (1/eV)
(E - E$_V$) (eV)

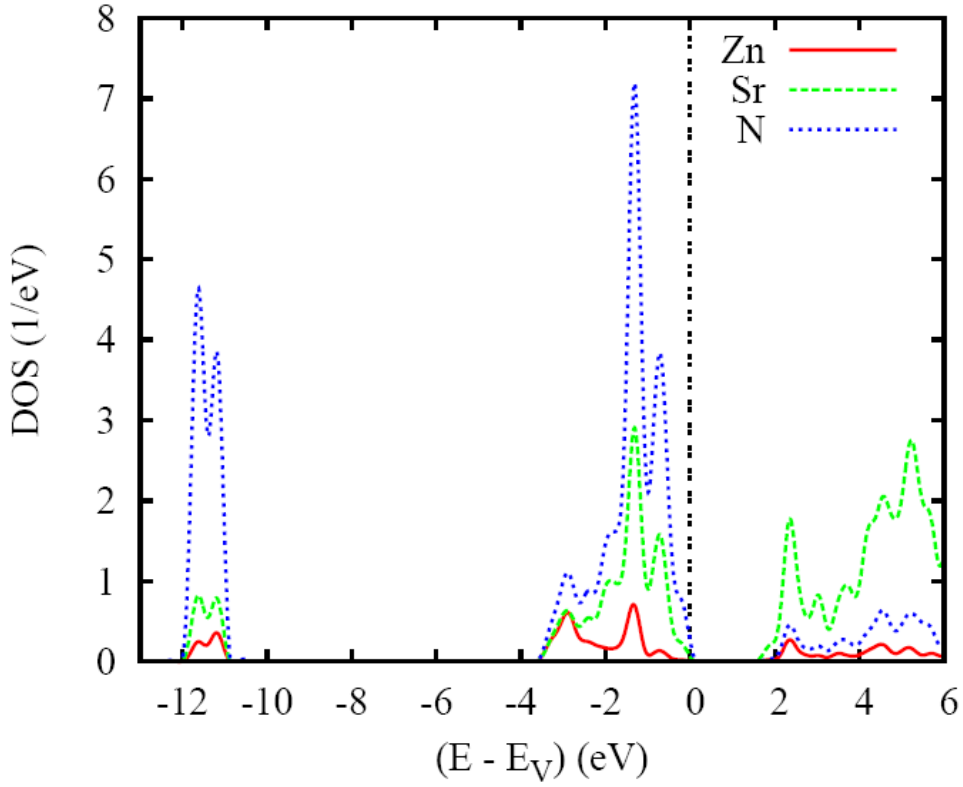
Zn
Sr
N
DOS (1/eV)
(E - E$_V$) (eV)

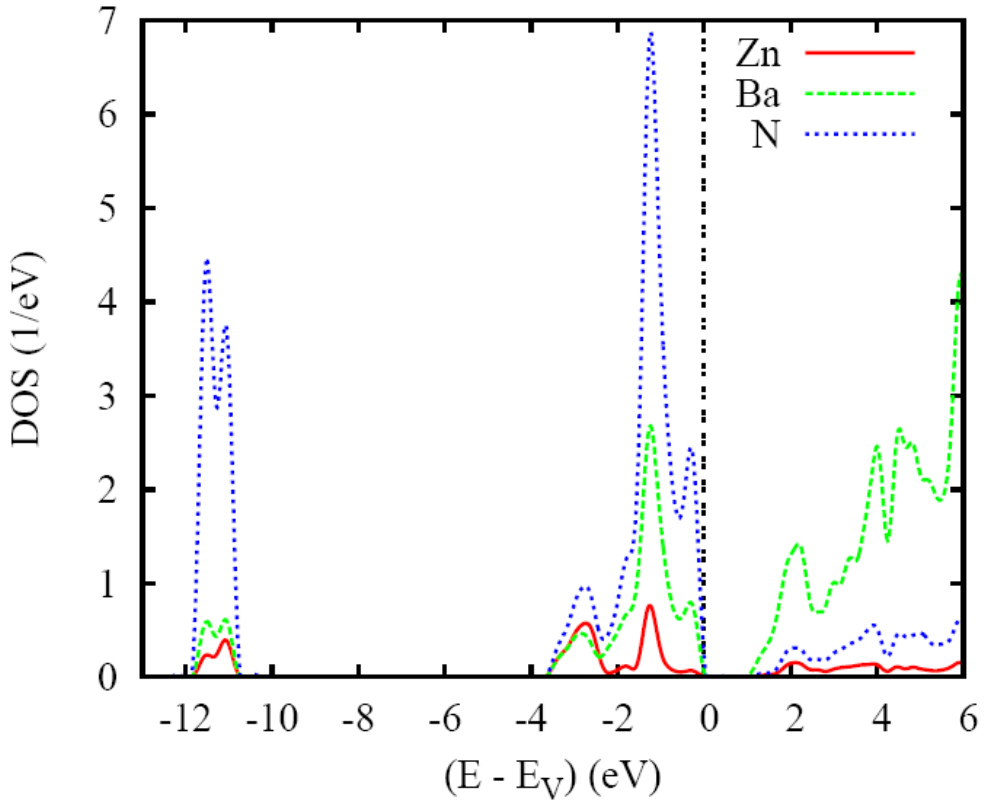

Fig. 3: AE_2ZnN_2: Site projected DOS for *AE*= Ca (top), *AE*= Sr (middle) and *AE*= Ba (bottom).

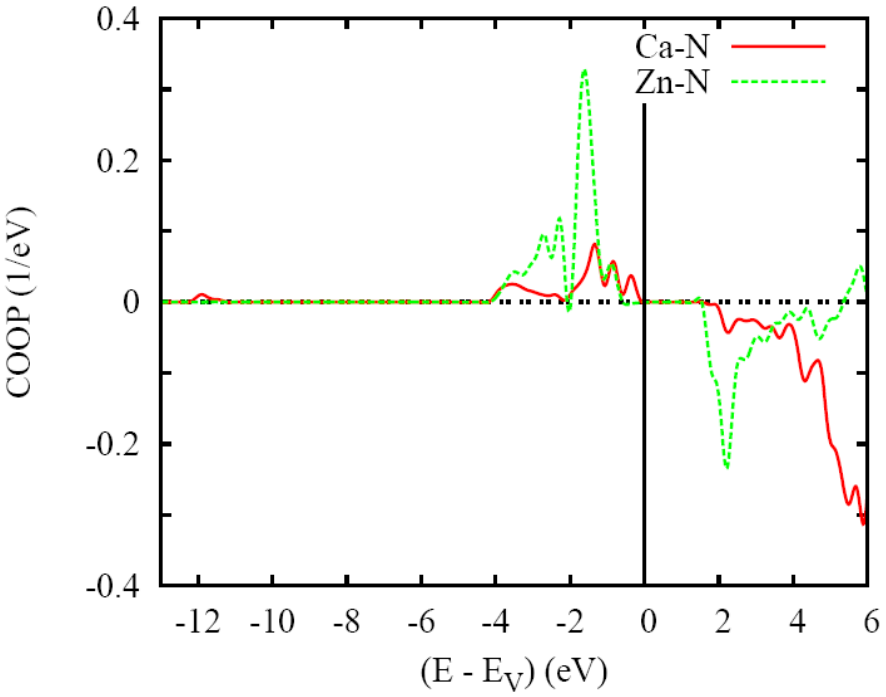
Ca-N
Zn-N
COOP (1/eV)
0.4
0.2
0
-0.2
-0.4
-12
-10
-8
-6
-4
-2
0
2
4
6
(E - E$_V$) (eV)

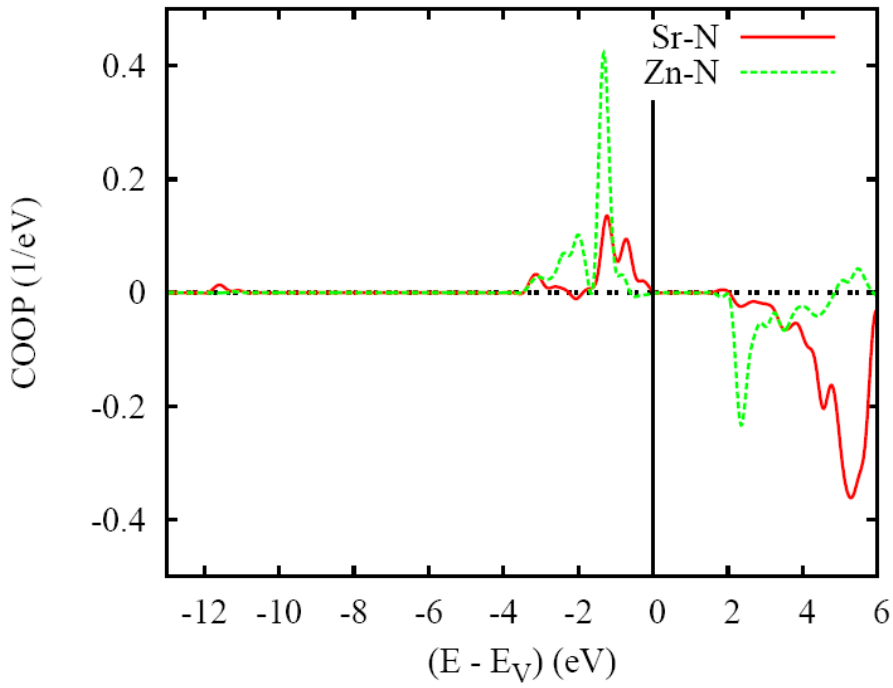
Sr-N
Zn-N
COOP (1/eV)
0.4
0.2
0
-0.2
-0.4
-12
-10
-8
-6
-4
-2
0
2
4
6
(E - E$_V$) (eV)

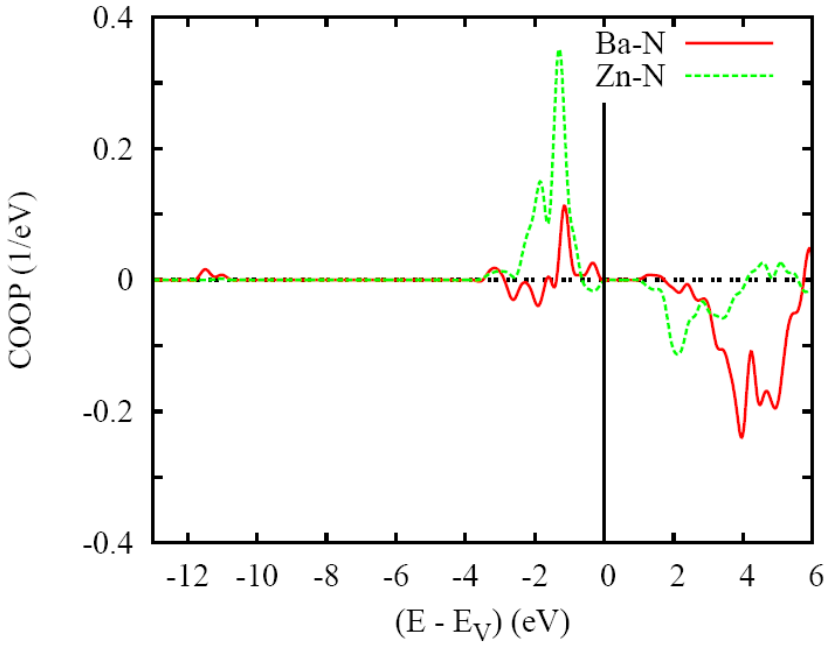

Fig. 4: AE_2ZnN_2, *AE* =Ca (top), Sr (middle), Ba (bottom): Atom-to-atom bonding magnitudes between *AE*-N and Zn-N.